

# Characterization of multilayered Ti/TiN films grown by chemical vapor deposition

J.C. Hu<sup>a</sup>, T.C. Chang<sup>b,\*</sup>, L.J. Chen<sup>a</sup>, Y.L. Yang<sup>b</sup>, C.Y. Chang<sup>c</sup>

<sup>a</sup>Department of Materials Science and Engineering, National Tsing Hua University, Hsinchu 300, Taiwan

<sup>b</sup>National Nano Device Laboratory, Hsinchu 300, Taiwan

<sup>c</sup>Department of Electronics Engineering and Institute of Electronics, National Chiao Tung University, Hsinchu 300, Taiwan

## Abstract

The resistivity of multilayered Ti/TiN films grown by chemical vapor deposition can be reduced from 240  $\mu\Omega$  cm (standard sample) to 120  $\mu\Omega$  cm with  $\text{NH}_3$  plasma post-treatment for 300 s. Increasing the number of multilayered Ti/TiN films of reduced thickness and a plasma post-treatment technique contributed to reducing the resistivity of TiN films effectively. Smooth multilayered Ti/TiN films were observed by XTEM image. The content of chlorine in the multilayered Ti/TiN film was 1.6 at.%. Therefore, corrosion in the subsequent Al film should be minimized. SIMS depth profiles of the multilayered Ti/TiN sample showed that Ti atom distribution is fairly uniform. The result is in agreement with the observation of XTEM and the measurement of AES depth profiles. The resistivity of multilayered Ti/TiN films can be further reduced to 75  $\mu\Omega$  cm with an in situ  $\text{NH}_3$  plasma post-treatment (500 W) for 300 s followed by RTA at 900°C for 60 s. Therefore, low resistivity (<100  $\mu\Omega$  cm) and low Cl concentration (<2 at.%) CVD TiN films can be achieved by a combination of forming a multilayered Ti/TiN structure, and using  $\text{NH}_3$  plasma post-treatment and RTA. © 1998 Elsevier Science S.A. All rights reserved.

**Keywords:** Multilayered Ti/TiN film; Plasma post-treatment; PECVD Ti; LPCVD TiN

## 1. Introduction

The microelectronics industry has shown an increasing interest in CVD TiN because of its high thermal stability, low electrical resistivity, and good diffusion barrier characteristics [1–3]. As the device dimensions scale down to deep submicron level, the limitation of films produced by physical vapor deposition has become apparent. Low pressure chemical vapor deposition (LPCVD) of TiN films provided excellent step coverage and uniformity [4,5], even for 0.5  $\mu\text{m}$  or smaller contact windows. The improved feature was attributed to favorable surface controlled reactions.

Two organometallic precursors of tetrakis dimethyl amino titanium (TDMAT) and tetrakis diethyl amino titanium (TDEAT) [6,7] were commonly used to deposit MOCVD TiN film. However, deposition of MOCVD TiN by thermal decomposition of TDMAT and TDEAT resulted in high carbon content, which was difficult to eliminate. Thus, the resistivity of MOCVD-TiN film was too high. By using  $\text{TiCl}_4$  and  $\text{NH}_3$  as reactants with  $\text{N}_2$  as a dilute gas, CVD-TiN films could be used as a diffusion barrier for Al interconnects and an adhesion layer for W-plugs.

In  $\text{TiCl}_4/\text{NH}_3$  based CVD-TiN process, the incorporation of chlorine (Cl) in the film is of major concern for long-term reliability of the finished device. Suzuki et al. [8] reported that a higher deposition temperature (>600°C) could reduce Cl concentration in a conventional thermal CVD-TiN film. Hence, LPCVD TiN film can be used as a barrier layer between Si and Al interconnections. Furthermore, in order to reduce chlorine content of TiN films, an in situ  $\text{NH}_3$  plasma post-treatment technique was applied [9]. As a result, the resistivity of TiN film can be reduced to 133  $\mu\Omega$  cm by in situ  $\text{NH}_3$  plasma post-treatment. In a previous study [10], rapid thermal annealing (RTA) of TiN was found to induce little grain growth, but promote sintering to eliminate grain boundary voids.

In the present work, a combination of multilayered Ti/TiN and plasma post-treatment technique was found to reduce the resistivity and concentration of chlorine in TiN films. In addition, multilayered Ti/TiN films processed by RTA were also characterized.

## 2. Experimental procedures

Single crystal, 15–25  $\Omega$  cm, 6-inch in diameter, p-type (001) oriented silicon wafers were used in this work. The wafers were first chemically cleaned by a conventional wet

\* Corresponding author Tel.: +886 3 5726100 X7710; fax: +00 886 3 5713403; e-mail: tcchang@mail.ndl.nctu.edu.tw.

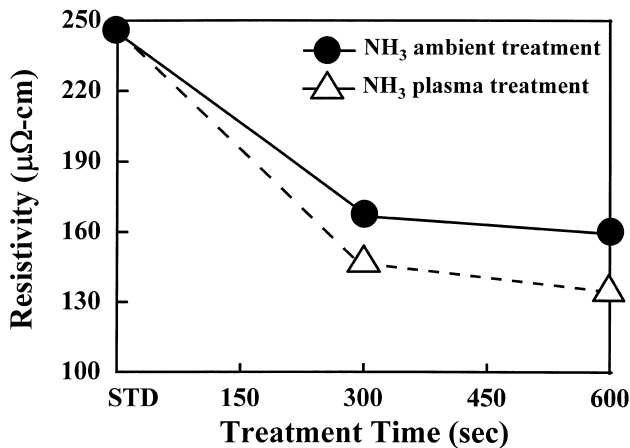


Fig. 1. The resistivity as a function of the post-treatment time for samples with different treatment methods. The thickness of these samples is 46 nm.

cleaning process. After initial cleaning, the wafers were dipped in a dilute HF solution (HF/H<sub>2</sub>O, 1:50) immediately before loading into a deposition chamber. The base vacuum level of the CVD chamber was maintained to be better than  $10^{-6}$  Torr. Plasma-enhanced chemical vapor deposition (PECVD) Ti and low-pressure chemical vapor deposition (LPCVD) TiN were deposited on the Si substrate in sequence. Ti films were deposited by PECVD using TiCl<sub>4</sub> and H<sub>2</sub> as reactants and the total pressure was 5 Torr. The RF power was 500 W. On the other hand, TiN films were deposited by LPCVD using TiCl<sub>4</sub> and NH<sub>3</sub> as reactants and the total pressure was 20 Torr when LPCVD TiN film was deposited. All the films were deposited by CVD processed in a Materials Research Corporation (MRC) multichamber cluster tool. The substrate temperature during both Ti and TiN film growth was maintained at 630°C. The in situ NH<sub>3</sub> plasma post-treatment was applied to as-deposited multi-

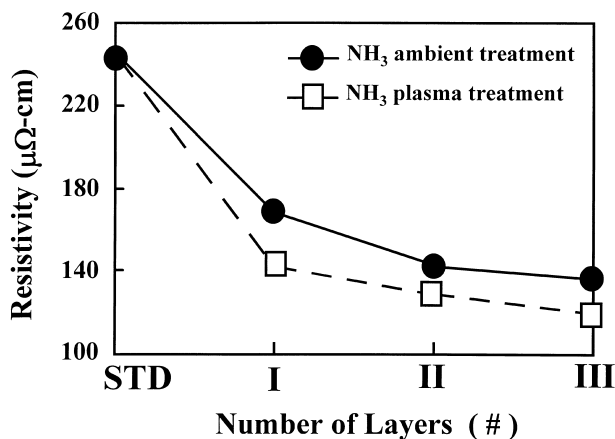


Fig. 2. The resistivity of various samples with different treatments. They are treated by in situ NH<sub>3</sub> ambient or NH<sub>3</sub> plasma post-treatment for 300 s. Samples are labeled as follows: (STD): TiN/TiSi<sub>2</sub>/Si, as a standard treated by in situ NH<sub>3</sub> ambient post-treatment for 30 s; (I): TiN/Ti/TiN/TiSi<sub>2</sub>/Si, (II): TiN/Ti/TiN/Ti/TiN/TiSi<sub>2</sub>/Si and (III): TiN/Ti/TiN/Ti/TiN/Ti/TiN/TiSi<sub>2</sub>/Si.

layered Ti/TiN films. The RF power for the NH<sub>3</sub> plasma post-treatment was 500 W. The TiN/TiSi<sub>2</sub>/Si sample was used as a standard. It was treated by NH<sub>3</sub> ambient post-treatment for 30 s, was labeled as STD. In addition, the multilayered TiN/Ti/TiN/TiSi<sub>2</sub>/Si, TiN/Ti/TiN/Ti/TiN/TiSi<sub>2</sub>/Si, and TiN/Ti/TiN/Ti/TiN/Ti/TiN/TiSi<sub>2</sub>/Si samples treated by NH<sub>3</sub> plasma post-treatment for 300 s were labeled as (I), (II) and (III), respectively. The total thickness of these multilayered Ti/TiN films was the same as the STD sample. Multilayered Ti/TiN films were deposited by PECVD Ti and LPCVD TiN, respectively. The deposition times of PECVD Ti on Si and TiN films were 60 and 20 s, respectively. Multilayered Ti/TiN samples processed by RTA were also investigated. All the multilayered Ti/TiN samples were annealed for 60 s in the temperature range of 650 to 900°C by RTA in N<sub>2</sub> ambient.

Transmission electron microscopy (TEM) and X-ray diffractometry (XRD) were applied to investigate the microstructure and crystal orientation of TiN films. Auger electron spectroscopy (AES) was used to determine the stoichiometry and uniformity along the depth direction. Secondary ion mass spectrometry (SIMS) was employed to characterize prepared samples. A four-point probe detector was used to measure the resistivity of samples with thickness 46 nm.

### 3. Results and discussion

PECVD Ti and LPCVD TiN were deposited on the Si substrate in sequence. Fig. 1 shows the resistivity of these multilayered samples as a function of the two post-treatments time. The resistivity of these samples decreased with the time of NH<sub>3</sub> post-annealing and NH<sub>3</sub> plasma post-treatment. The resistivity of these films was reduced from 240 to 133 μΩ cm after NH<sub>3</sub> plasma-treatment for 600 s. However, the resistivity of these films was only reduced to 160 μΩ cm after thermal annealing in NH<sub>3</sub> ambient. Therefore, in situ NH<sub>3</sub> plasma post-treatment was more effective in reducing the resistivity of TiN films [9]. In addition, selective NH<sub>3</sub> plasma post-treatment for 300 s can save processing time. For the investigation of multilayered Ti/TiN films, PECVD Ti and multilayered Ti/TiN were also deposited on the Si substrate in sequence. The substrate temperature during Ti and TiN film growth was also maintained at 630°C. A 9.5-nm thick TiSi<sub>2</sub> thin film was formed during the deposition of PECVD Ti on Si. Then a 46-nm thick multilayered Ti/TiN thin film was deposited on TiSi<sub>2</sub>/Si. Both in situ NH<sub>3</sub> post-annealing and in situ NH<sub>3</sub> plasma post-treatment for 300 s were carried out to reduce Cl and compensate N concentration in multilayered Ti/TiN films. Fig. 2 shows the resistivity of these samples as a function of the number of layers. The resistivity of these samples was decreased with the number of Ti/TiN layers. The resistivity of these multilayered Ti/TiN films can be reduced from 240 (STD) to 120 μΩ cm (III) with NH<sub>3</sub> plasma-treatment for

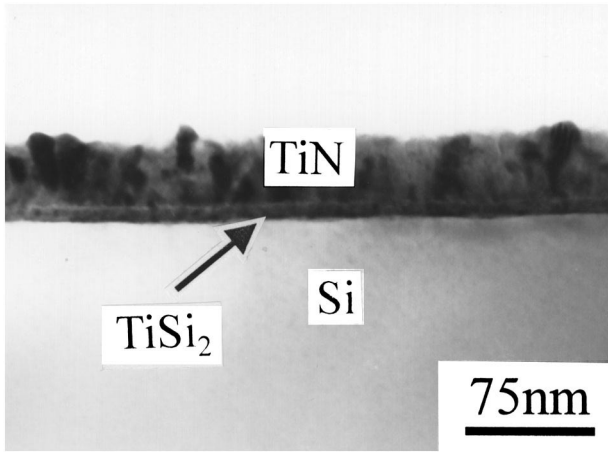


Fig. 3. XTEM image of a CVD-TiN/TiSi<sub>2</sub>/Si sample treated by in situ NH<sub>3</sub> plasma post-treatment for 600 s. The RF power of NH<sub>3</sub> plasma was 500 W. The thickness of the CVD-TiN sample is 46 nm.

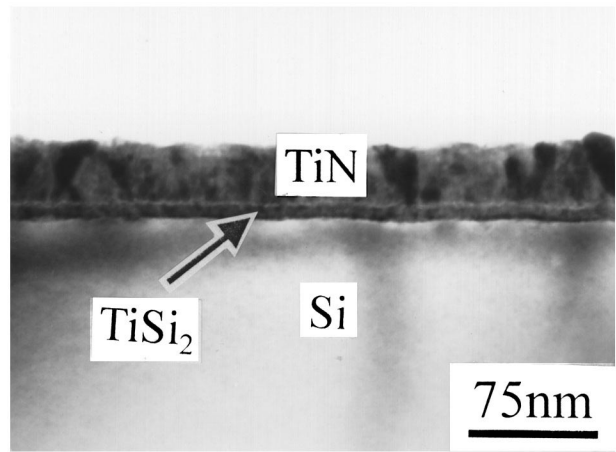


Fig. 5. XTEM image of a multilayered TiN/Ti/TiN/Ti/TiN/Ti/TiN/TiSi<sub>2</sub>/Si sample treated by in situ NH<sub>3</sub> plasma post-treatment for 300 s. The RF power of NH<sub>3</sub> plasma was 500 W. The thickness of the multilayered Ti/TiN sample is 46 nm.

300 s. Therefore, increasing the number of multilayered of Ti/TiN films and utilizing the plasma post-treatment technique contributed to reduce the resistivity of TiN films.

A cross-section TEM image of TiN film treated by NH<sub>3</sub> plasma for 600 s is shown in Fig. 3. The interfaces of TiN/TiSi<sub>2</sub>/Si structure are seen to be rather smooth. Fig. 4 shows a plan-view micrograph. The average grain size of TiN film was measured to be about 20 nm. For multilayered Ti/TiN films, a cross-section TEM image of TiN/Ti/TiN/Ti/TiN/Ti/TiN/TiSi<sub>2</sub>/Si sample was treated by an in situ NH<sub>3</sub> plasma post-treatment for 300 s which was labeled as sample (III). The interfaces of multilayered Ti/TiN/TiSi<sub>2</sub>/Si are also seen to be rather smooth as seen in Fig. 5. However, the interfaces of multilayered Ti/TiN in TiN films are not apparent in the XTEM image. It is believed that Ti atoms are distributed fairly uniformly by fast diffusion in TiN films. A plan-view micrograph is shown in Fig. 6. The average grain size of multilayered Ti/TiN film was also about 20 nm.

Fig. 7 shows the AES depth profile of a TiN/TiSi<sub>2</sub>/Si sample after NH<sub>3</sub> ambient post-treatment for 30 s. The concentration of Cl in the sample was found to be about 3 at.%. Therefore, the sample STD had a higher value of resistivity (~240 μΩ cm). In contrast, Fig. 8 reveals the AES depth profile of TiN/Ti/TiN/Ti/TiN/Ti/TiN/TiSi<sub>2</sub>/Si sample after being treated by NH<sub>3</sub> plasma post-treatment for 300 s. The concentration of Cl in the sample was found to be about 1.6 at.%, which was lower than that of the sample STD. A previous study showed that chlorine content in excess of 5 at.% would degrade metal reliability and increase the resistivity of the TiN film [11]. The content of chlorine in the multilayered Ti/TiN film was chosen to be 1.6 at.%. Therefore, corrosion in subsequent Al film should be eliminated. In addition, the concentration of Ti+N was

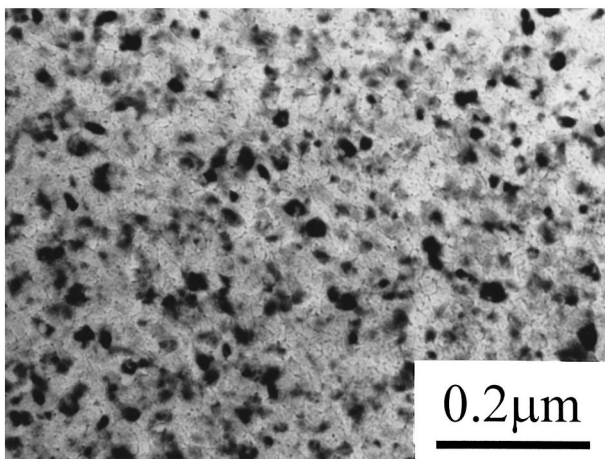


Fig. 4. Plan-view image of a CVD-TiN sample treated by in situ NH<sub>3</sub> plasma post-treatment for 600 s. The RF power of NH<sub>3</sub> plasma was 500 W. The thickness of the CVD-TiN sample is 46 nm.

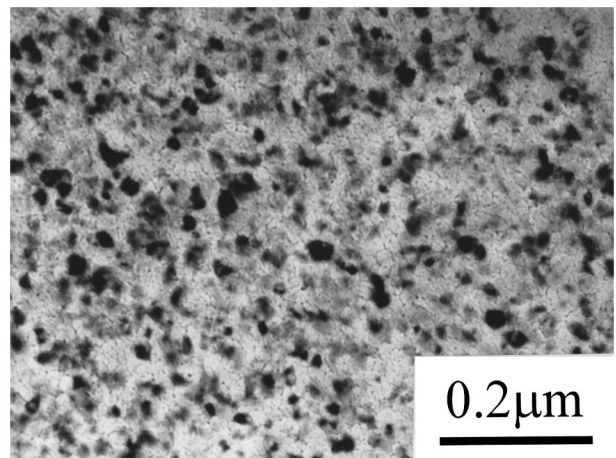


Fig. 6. Plan-view image of a multilayered TiN/Ti/TiN/Ti/TiN/Ti/TiN/TiSi<sub>2</sub>/Si sample treated by in situ NH<sub>3</sub> plasma post-treatment for 300 s. The RF power of NH<sub>3</sub> plasma was 500 W. The thickness of the multilayered Ti/TiN sample is 46 nm.

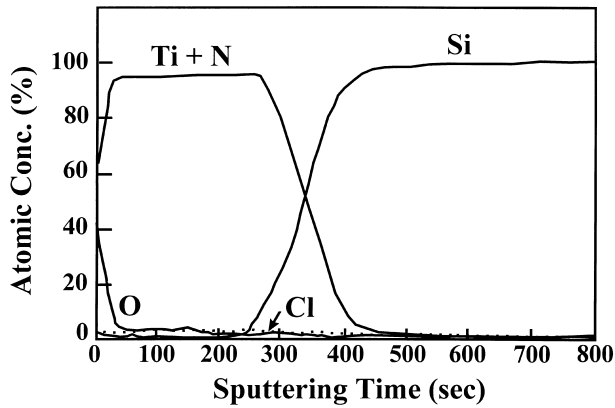


Fig. 7. The AES depth profile of a CVD-TiN/TiSi<sub>2</sub>/Si sample after being treated by in situ NH<sub>3</sub> ambient post-treatment for 30 s.

fairly uniformly in the TiN/Ti/TiN/Ti/TiN/Ti/TiN/TiSi<sub>2</sub>/Si sample by AES measurement.

To investigate Ti atom distribution behavior in multilayered Ti/TiN films in detail, the <sup>47</sup>Ti+N and <sup>51</sup>Ti depth profiles were measured by SIMS for an as-deposited multilayered TiN/Ti/TiN/Ti/TiN/Ti/TiN/TiSi<sub>2</sub>/Si sample as shown in Fig. 9. It can be seen that the distribution of Ti atoms is fairly uniform in the multilayered Ti/TiN sample. The result is in agreement with the observation of XTEM and the measurement of AES depth profile shown in Fig. 5 and Fig. 6. On the other hand, a previous study showed that the PECVD Ti deposition rate varied with different substrate [12]. Except for amorphous and crystal Si, the deposition rate of PECVD Ti is rather low on other substrates. Owing to the TiCl<sub>4</sub> etching characteristics, deposition and etching behavior can occur simultaneously for PECVD Ti deposited on TiN films. As a result, the thickness of PECVD Ti deposited on TiN for 20 s to form multilayered Ti/TiN films is relatively thin. Furthermore, the Ti atoms are fairly uniformly distributed by fast diffusion in TiN films. In addition, the very thin layer of PECVD Ti deposited on TiN may

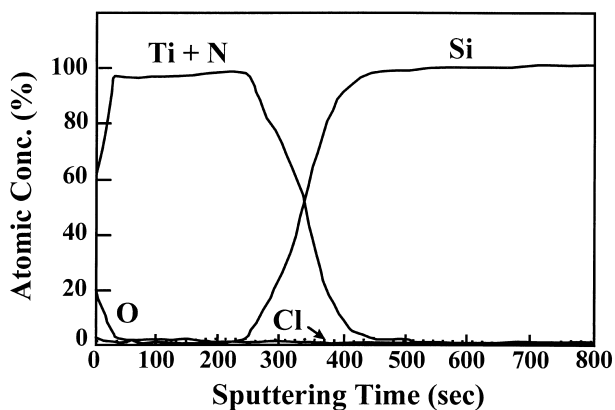


Fig. 8. The AES depth profile of a multilayered TiN/Ti/TiN/Ti/TiN/Ti/TiN/TiSi<sub>2</sub>/Si sample treated by in situ NH<sub>3</sub> plasma post-treatment for 300 s.

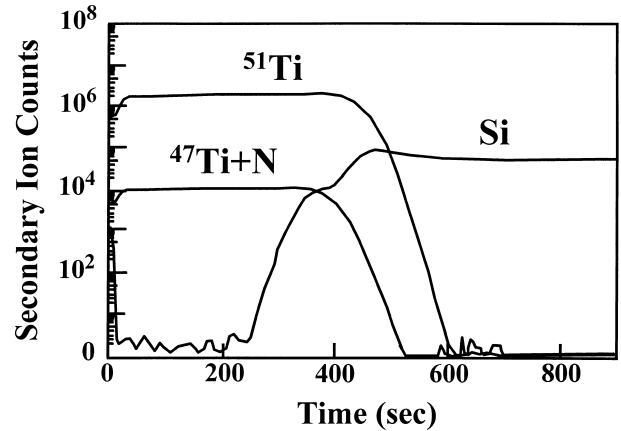


Fig. 9. The SIMS depth profile of a multilayered TiN/Ti/TiN/Ti/TiN/Ti/TiN/TiSi<sub>2</sub>/Si sample treated by in situ NH<sub>3</sub> plasma post-treatment for 300 s.

also fill the grain boundary of TiN film to improve resistivity.

Fig. 10 shows the resistivity of these multilayered Ti/TiN samples as a function of RTA temperature in samples annealed for 60 s. The resistivity of these multilayered TiN/Ti/TiN/Ti/TiN/Ti/TiN/TiSi<sub>2</sub>/Si samples can be reduced to 75 μΩ cm with a NH<sub>3</sub> plasma post-treatment for 300 s followed by RTA at 900°C for 60 s. However, the resistivity of TiN films STD was only reduced to 150 μΩ cm with annealing in a NH<sub>3</sub> ambient post-treatment for 30 s followed by RTA at 900°C for 60 s. A previous study [10] showed that the RTA-induced grain sintering results in a tighter grain boundary structure and thus enhances the TiN barrier properties, which is of great importance for the sub-0.25 μm technology with Al plug or Cu metallization. In addition, XRD peaks of multilayered TiN/Ti/TiN/Ti/TiN/Ti/TiN/TiSi<sub>2</sub>/Si film reveal a polycrystalline phase of NaCl type is seen in Fig. 11. A stronger (002) and a weak (111) peak

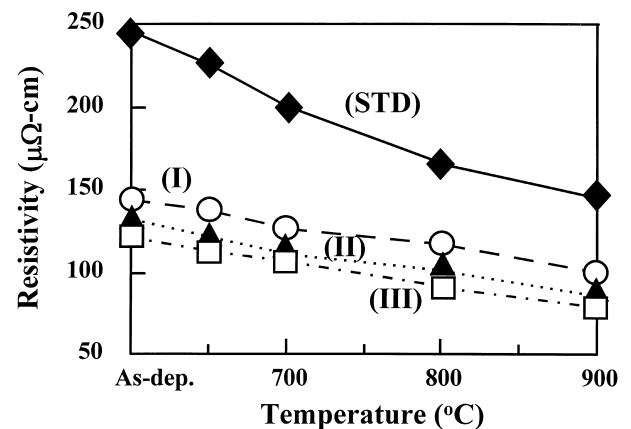


Fig. 10. The resistivity of various samples as a function of RTA temperature for 60 s. Samples are labeled as follows: (STD): TiN/TiSi<sub>2</sub>/Si, as a standard treated by in situ NH<sub>3</sub> ambient post-treatment for 30 s; (I): TiN/Ti/TiN/TiSi<sub>2</sub>/Si, (II): TiN/Ti/TiN/Ti/TiN/TiSi<sub>2</sub>/Si and (III): TiN/Ti/TiN/Ti/TiN/Ti/TiN/TiSi<sub>2</sub>/Si. They were treated by in situ NH<sub>3</sub> ambient or NH<sub>3</sub> plasma post-treatment for 300 s.

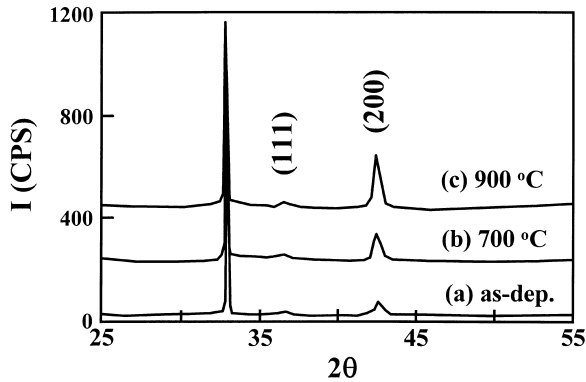


Fig. 11. XRD spectra of multilayered TiN/Ti/TiN/Ti/TiN/Ti/TiN/TiSi<sub>2</sub>/Si samples treated by in situ NH<sub>3</sub> plasma post-treatment for 300 s followed by RTA treatment for 60 s. The wavelength of the CuK $\alpha$  X-ray is 0.15405 nm.

in XRD spectrum of multilayered TiN/Ti/TiN/Ti/TiN/Ti/TiN/TiSi<sub>2</sub>/Si film by RTA at 900°C for 60 s were observed. Due to grain growth, the intensity of (002) and (111) peaks of the XRD spectrum of multilayered TiN/Ti/TiN/Ti/TiN/Ti/TiN/TiSi<sub>2</sub>/Si film increased with RTA temperature. Fig. 12 shows the grain structure of multilayered TiN/Ti/TiN/Ti/TiN/Ti/TiN/TiSi<sub>2</sub>/Si film after RTA at 900°C for 60 s. The average grain size was measured to be about 35 nm which is larger than that of as-deposited multilayered TiN/Ti/TiN/Ti/TiN/Ti/TiN/TiSi<sub>2</sub>/Si film (20 nm). As a result, low resistivity (<100  $\mu\Omega$  cm) and low Cl concentration (<2 at.%) of CVD TiN films can be achieved by a combination of forming multilayered Ti/TiN structure, NH<sub>3</sub> plasma post-treatment and RTA.

#### 4. Conclusions

The resistivity of multilayered Ti/TiN films can be reduced from 240 cm (standard sample) to 120  $\mu\Omega$  cm with NH<sub>3</sub> plasma post-treatment for 300 s. Increasing the number of multilayered Ti/TiN films and the use of the plasma post-treatment technique contributed to reduce the resistivity of TiN films effectively. Smooth multilayered Ti/TiN films were observed by XTEM image. The content of chlorine in the multilayered Ti/TiN film was 1.6 at.%. Therefore, corrosion in the subsequent Al film should be minimized. SIMS depth profiles of the multilayered Ti/TiN sample showed that Ti atom distribution is fairly uniform. This result is in agreement with the observation of XTEM and the measurement of AES depth profile. The resistivity of multilayered Ti/TiN films can be further reduced to 75  $\mu\Omega$  cm with a NH<sub>3</sub> plasma post-treatment for 300 s followed by RTA at 900°C for 60 s. Therefore, low resistivity (<100  $\mu\Omega$  cm) and low Cl concentration

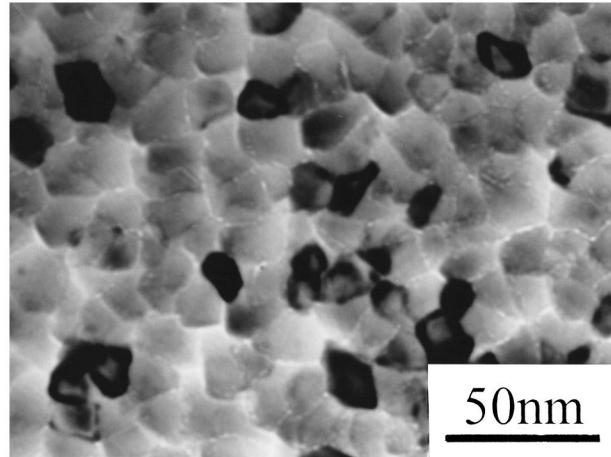


Fig. 12. Plan-view image of multilayered TiN/Ti/TiN/Ti/TiN/Ti/TiN/TiSi<sub>2</sub>/Si sample treated by in situ NH<sub>3</sub> plasma post-treatment for 300 s followed by RTA at 900°C for 60 s.

(<2 at.%) of CVD TiN films can be achieved by a combination of forming multilayered Ti/TiN structure, and using NH<sub>3</sub> plasma post-treatment and RTA.

#### Acknowledgements

The work was supported by National Nano Device Laboratory and National Science Council of the People's Republic of China under contract nos. NSC87-2215-E317-002 and NSC87-2721-2317-200.

#### References

- [1] R.I. Hedge, R.W. Fiordalice, E.O. Travis, R.J. Tobin, *J. Vac. Sci. Technol. B* 11 (1993) 1287.
- [2] J.S. Byun, C.R. Kim, K.G. Rha, J.J. Kim, *Jpn. J. Appl. Phys.* 34 (1995) 978.
- [3] J.T. Hillman, R. Foster, J. Faguet, W. Triggs, R. Arora, M. Ameen, *Solid State Technol.* (1995) 147.
- [4] J.T. Hillman, *Proc. SEMI Taiwan Tech. Conf.*, Taiwan p. (1995) 8.
- [5] J. Faguet, C. Arena, E. Guidotti, R.F. Foster, J.T. Hillman, *Advanced Metallization for ULSI Applications in 1995. Mater. Res. Stand.*, 1995, p. 259.
- [6] A. Paranipe, M.L. Raja, *J. Vac. Sci. Technol. B* 13 (1995) 2105.
- [7] S.C. Sun, M.H. Tsai, *Thin Solid Films* 253 (1994) 440.
- [8] T. Suzuki, T. Ohba, Y. Furumura, H. Tsutikawa, *Proc. 10th Int. VLSI Multilevel Interconnection Conf.*, IEEE, New York, 1993 p. 418.
- [9] Y.J. Mei, T.C. Chang, J.C. Hu, et al., *Thin Solid Films* 308 (1997) 594.
- [10] X.W. Lin, S. Bothra, L. Topete, D. Pramanik, *14th Int. VLSI Multilevel Interconnection Conf.*, 1997 p. 443.
- [11] T. Kaizuka, H. Shinriki, N. Takeyasu, T. Ohta, *Jpn. J. Appl. Phys.* 33 (1994) 470.
- [12] T. Taguwa, K. Urabe, K. Ohto, H. Gomi, *14th Int. VLSI Multilevel Interconnection Conf.*, 1997 p. 255.